Journal of Hydrology: Regional Studies 44 (2022) 101201

Contents lists available at ScienceDirect

Journal of Hydrology: Regional Studies

journal homepage: www.elsevier.com/locate/ejrh

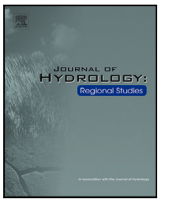

Precipitation trends in North and South Carolina, USA

Giacomo Moraglia [a,*], Erika Brattich [b], Gregory Carbone [c]

[a] Department of Civil & Environmental Engineering & Earth Sciences, College of Engineering, University of Notre Dame, Notre Dame, IN 46556, USA

[b] Department of Physics and Astronomy "Augusto Righi", Alma Mater Studiorum Università di Bologna, 40126, Bologna, Italy

[c] Department of Geography, College of Arts and Sciences, University of South Carolina, Columbia, SC 29208, USA

ARTICLE INFO

Keywords:
Climate change
Rainfall
United states
Climatology

ABSTRACT

Study region

North and South Carolina, USA.

Study focus

Intense precipitation poses risks to life and property. Its frequency can change in response to global-scale drivers, but its spatial expression can vary seasonally and regionally, and be dependent on how it is measured and what analysis period is used. We investigate forty-four historical stations from the U.S. Historical Climatology Network (USHCN) across North and South Carolina to determine trends in the pluviometric regime defined by the Expert Team on Climate Change Detection and Indices (ETCCDI).

New hydrological insights for the region

Most of the stations in this area do not display consistent, statistically significant trends across the suite of ETCCDI measures of precipitation amount, frequency, and intensity. In addition, the direction, spatial patterns and cross seasonal results are not consistent for the small number of stations that do show a trend in annual or seasonal precipitation totals. A third of stations have a statistically significant increasing trend in the annual number of light rain days; these generally match those with a statistically significant trend in wet days. Relatively few stations, typically around 10 per cent, have statistically significant trends in precipitation intensity measures. Notable exceptions include 2- and 5-day fall maximum precipitation values. Our findings contribute to a broader literature regarding trends in the southeastern United States (SEUS) and have significant relevance in adaptation planning that seeks to understand the relative contribution of multiple causes of natural hazards.

1. Introduction

Increased precipitation intensity is one of many potential impacts of global climate change, one that presents risks to life and property as well as challenges to infrastructure planning and risk/disaster management [IPCC (2012)]. As the planet warms, atmospheric moisture-holding capacity should increase, following the Clausius–Clapeyron equation (C-C), at 7% per °C (Trenberth et al., 2003). Recent research has documented connections between moisture availability and increases in observed precipitation intensity using the empirical record or model simulations at global, continental, and regional scales (O'Gorman and Schneider, 2009; Fischer and Knutti, 2015; Forestieri et al., 2018; Huang et al., 2017; Grabowski, 2019; Kunkel et al., 2020a,b; Tabari, 2020).

* Corresponding author.
E-mail address: gmoragli@nd.edu (G. Moraglia).

https://doi.org/10.1016/j.ejrh.2022.101201
Received 22 September 2021; Received in revised form 26 July 2022; Accepted 3 September 2022
Available online 5 October 2022

In the southeastern United States (SEUS), moisture content controls on precipitation intensity have been generally consistent with the C–C relationship (Easterling et al., 2013; Ivancic and Shaw, 2016). However, as in other regions, precipitation rates respond in a complex way, dependent on moisture availability, but also on stability changes, storm dynamics, and regional to local geography (Zhang et al., 2017). SEUS storm systems vary seasonally, and geographic features such as the proximity to warm water bodies and orography strongly influence heavy precipitation events. In the cool season, heavy precipitation is typically caused by mid-latitude cyclones or associated fronts; their frequency and magnitude is influenced by El Niño Southern Oscillation (ENSO) phase (Ropelewski and Halpert, 1986; Gershunov and Barnett, 1998). During the warm season, intense precipitation events are typically driven by tropical systems or slow-moving convective cells (Konrad, 2001; Shepherd et al., 2007; Knight and Davis, 2009; Konrad and Perry, 2009; Kunkel et al., 2012; Skeeter et al., 2018). This complexity could lead to large spatial variations in precipitation scaling across the SEUS. In addition to the complexity of causation, the very measure of precipitation intensity presents challenges (Pendergrass, 2018). While a variety of standards are recognized (Zhang et al., 2011a; Alexander et al., 2006, 2019), only a few previous studies considered a wide suite of metrics across long time frames such as those documented here. Specifically, the investigation presented herein is to our knowledge unprecedented in the SEUS with respect to record length, number of stations, and number of precipitation measures.

Prior research documenting the nature of precipitation intensity changes in the SEUS reveals the challenges associated with its measurement, and shows how choice of metric (e.g., measures of precipitation frequency, duration, or intensity), analysis period, spatial extent, and season can influence results (Bishop et al., 2019; Brown et al., 2019; Powell and Keim, 2015; Skeeter et al., 2018; Kam et al., 2014; Diem, 2013). Several findings emerge from this work. First, in the post-World War II era, precipitation intensity increased in many parts of the Southeast. For example, Powell and Keim (2015) show 1948–2012 increases in several of the Expert Team on Climate Change Detection and Indices (ETCCDI) for precipitation intensity (Alexander et al., 2006). Kunkel et al. (2020a) document increases, from 1949 to 2016, in 1- to 5-day accumulation for events with an estimated 1- to 5-year recurrence interval. Easterling et al. (2017) show a 49% regional increase in the number of 5-year, 2-day precipitation events, and a 27% increase in 99th-percentile events from 1958 to 2016. Second, the results for trends extending from the early 20th century are less definitive. Using 1901–2016 data, Easterling et al. (2017) found a 16% increase in the 1-day precipitation maxima expected every five years, and a 58% increase in the number of 5-year, 2-day events. By contrast, Kunkel et al. (2012) found no increasing trend in daily extremes for 1-in-5-year events in the Southeast using 1908–2009 data and subdividing trends by storm type. Similarly, Bonnin et al. (2011) found that the magnitude of Southeast precipitation intensity trends from 1908–2007 was small, particularly as measured against interannual and interdecadal variability. Third, results differ across seasons with the most pronounced increases observed in autumn (Easterling et al., 2017; Park Williams et al., 2017; Skeeter et al., 2018). Fourth, precipitation intensity trends vary spatially across the region. In particular, there are many stations in North and South Carolina with no precipitation intensity trend, or with smaller trends than stations further north or west, or when compared against results aggregated across the SEUS (Powell and Keim, 2015; Brown et al., 2019; Skeeter et al., 2018; Brown et al., 2020; Kunkel et al., 2020a).

This study explores the "Carolinas anomaly" expanding upon the best aspects of prior work by analyzing as many stations as possible across an extensive time period using a wide suite of metrics related to annual, seasonal, and monthly precipitation amounts, frequency, and intensity. Examining a smaller region allows us to take advantage of a longer record (Park Williams et al., 2017), and one that includes some of the geographic features (e.g., orography and coastal proximity) that influence heavy precipitation (Fig. 1). In addition, the use of a wide range of metrics allows us to explore inter-relationships between variables.

2. Data and methods

We used the Historical Climatology Network (USHCN) daily data set. The USHCN is derived predominantly from the National Oceanic and Atmospheric Administration (NOAA) Cooperative Observer Program (COOP) Network using sites selected for overall spatial coverage, record length, data completeness, and historical stability (NOAA, 2021). The USHCN is a high quality data set including basic meteorological variables from 1218 observing stations across the United States. The period of record varies for each station, but all USHCN stations must meet requirements regarding record length, percent missing data, number of station moves, and other changes affecting data homogeneity (Menne et al., 2006). Before performing statistical and trend analyses, the resulting dataset was subjected to a thorough quality check to identify outliers that could affect the trend analysis. To this end, the occurrence of record high precipitation in the dataset was carefully cross-checked and validated only if the observation was confirmed by records at a nearby station and/or relevant metadata (e.g., local or national news). Daily records from 44 stations in North and South Carolina were selected to maximize temporal and spatial coverage (Tables 1 and 2). Each record starts in approximately 1900 (two begin in the 1910s); most extend to 2019, the earliest ends in 1999. Since incomplete years affect trend estimates, we filtered out years with more than 30 missing days, i.e., including only those stations with less than 10% of missing daily records (Powell and Keim, 2015). Tables 1 and 2 summarize period of record, geographic coordinates, and total number of observations for each station in the two regions.

Our first analysis was designed to identify similarities in precipitation patterns in order to characterize subregions across the geography of the Carolinas. We selected seven reference stations spread geographically south to north and from the coast to the mountains, and with relatively complete records: Asheville, NC; Conway, SC; Effingham, SC; Hendersonville, NC; Randleman, NC; Walhalla, SC; and Willard, NC. We applied a Wilcoxon rank-sum test to detect similarity in monthly, seasonal, and annual precipitation between these reference stations and all remaining stations. Each station with a p-value of 0.05 (95th% confidence) or higher was identified as having no statistically significant difference with the reference station. This method yielded three logically

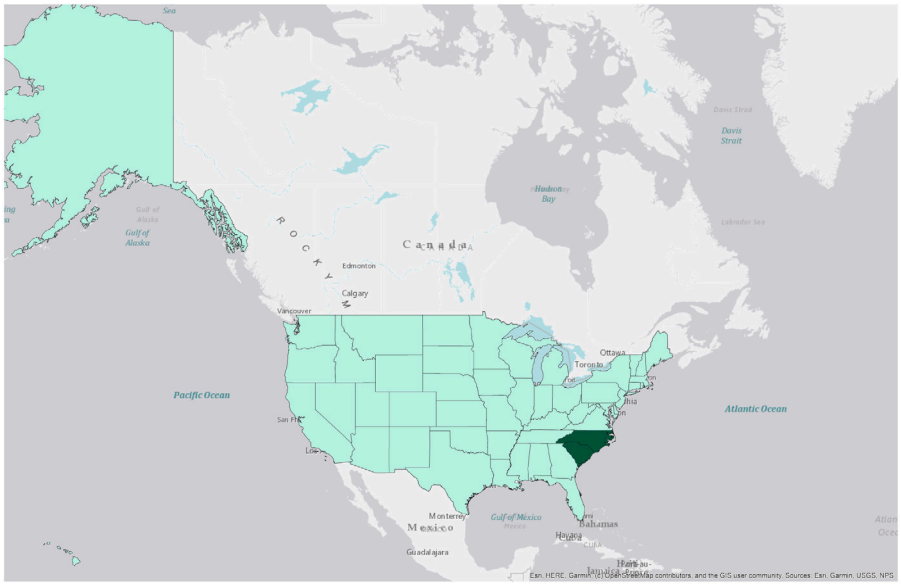

Fig. 1. Map of the United States depicting in dark green color the two Carolinas (North Carolina and South Carolina). (Source: OpenStreetMap contributors and the GIS user community.). (For interpretation of the references to color in this figure legend, the reader is referred to the web version of this article.)

Table 1
List of stations, with name, record length, coordinates, daily observations and number of years filtered out from the analysis selected from South Carolina USHCN network.

Station	Record	Lat (°)	Long (°)	Daily obs.	Years filtered out
Blackville 3 W	1900–1999	33.36306	−81.32917	35,017	3
Calhoun Falls	1900–2019	34.09050	−82.58830	41,422	6
Camden 3 W	1900–2001	34.24291	−80.65652	32,867	10
Catawba	1906–2019	34.85736	−80.91341	39,411	4
Chappells 2 NNW	1905–2012	34.21410	−81.88500	35,583	7
Clemson University	1900–2019	34.66036	−82.82325	42,724	3
Conway	1900–2014	33.83130	−79.05580	38,653	8
Darlington	1900–2019	34.30110	−79.87660	31,246	35
Effingham	1900–2012	34.06270	−79.75550	39,585	3
Georgetown 2 S E	1900–2005	33.36194	−79.22389	26,620	29
Greenwood	1900–2011	34.19970	−82.17110	35,787	12
Little Mountain	1900–2019	34.19950	−81.41436	40,847	8
Newberry	1900–2019	34.29165	−81.62089	33,488	28
Saluda	1903–2019	33.99185	−81.77129	35,055	19
Santuck	1900–2019	34.63500	−81.52050	40,533	9
Summerville 4 W	1900–2019	33.03660	−80.23250	35,782	16
Walhalla	1900–2019	34.75450	−83.07510	34,694	24
Winnsboro	1900–2019	34.37060	−81.08250	36,874	19
Winthrop University	1900–2019	34.93880	−81.03313	39,804	11
Yemassee 1 N	1900–2019	32.70190	−80.85180	39,019	12

organized regions representing coastal, central, and upstate portions of North and South Carolina. The main difference between these areas is a higher summer precipitation peak near the ocean, a winter peak in the upstate, and overall lower values in the central (inner-coastal plain and piedmont) region.

For precipitation intensity, duration, and frequency, we used the 10 ETCCDI core precipitation measures (Alexander et al., 2007; Zhang et al., 2011b) adding a few others following definitions specified below. Because changes in precipitation vary by season (Easterling et al., 2017), we conduct our analysis seasonally using the following standard: spring (March 1–May 31), summer (June 1–August 31), fall (September 1 –November 30) and winter (December 1–February 28/29). We calculated each index as follows:

2.0.1. Rx1day — Seasonal maximum 1-day precipitation

$$Rx1day_j = max(RR_{ij}) \tag{1}$$

where RR_{ij} is the daily precipitation amount on day i in season j.

Table 2
List of stations, with name, record length, coordinates, daily observations and number of years filtered out from the analysis selected from North Carolina USHCN network.

Station	Record	Lat (°)	Long (°)	Daily obs.	Years filters out
Asheville	1900–2019	35.59540	−82.55680	43,464	1
Banner Elk	1907–2019	36.16160	−81.87410	30,666	28
Chapel Hill 2 W	1900–2019	35.90860	−79.07940	33,306	26
Durham	1901–2013	36.04250	−78.96250	35,547	6
Edenton	1900–2019	36.01640	−76.55160	40,896	8
Elizabeth City	1912–2019	36.30960	−76.20500	33,207	16
Greenville	1900–2019	35.64000	−77.39840	34,672	11
Henderson 2 NNW	1900–2019	36.34880	−78.41193	38,998	12
Hendersonville 1 NE	1900–2019	35.32970	−82.44910	40,866	8
Kinston 7 SE	1900–2019	35.19670	−77.54320	33,930	23
Lumberton	1903–2019	34.62690	−79.02500	39,286	8
Marion	1900–2019	35.68470	−82.00840	32,803	8
Monroe 2 SE	1900–2019	34.97970	−80.52330	41,601	5
Mount Airy 2 W	1903–2019	36.49618	−80.65226	40,130	10
Murphy 4 ESE	1900–2019	35.07140	−83.96840	39,721	10
New Holland	1915–2002	35.44861	−76.21083	22,640	23
Randleman	1905–2019	35.82220	−79.79170	39,944	5
Salisbury	1900–2019	35.68360	−80.48220	38,661	13
Smithfield	1911–2019	35.51710	−78.34430	36,018	8
Southport 5N	1900–2016	33.99470	−78.00770	35,001	18
Statesville 2 NNE	1901–2019	35.80990	−80.88080	40,885	6
Tarboro 1 S	1900–2019	35.88413	−77.53857	37,971	14
Willard 4 SW	1908–2011	34.66050	−78.04540	34,659	25
Wilson 3 SW	1937–2011	35.69380	−77.94600	28,844	5

2.0.2. Rx2day — Seasonal maximum consecutive 2-day precipitation

$$Rx2day_j = max(RR_{kj}) \tag{2}$$

where RR_{kj} is the precipitation amount for the 2-day interval ending k, season j.

2.0.3. Rx5day — Seasonal maximum consecutive 5-day precipitation

$$Rx5day_j = max(RR_{kj}) \tag{3}$$

where RR_{kj} indicates the precipitation amount for the 5-day interval ending k, season j.

2.0.4. SDII — Simple precipitation intensity index

$$SDIIj = \frac{\sum RR_{wj}}{W}$$

where RR_{wj} is the daily precipitation amount on wet days in season j, and W represents the number of wet days in j.

2.0.5. CDD — Consecutive dry days

Maximum number of consecutive days with RR < 1 mm. Let RR_{ij} be the daily precipitation amount on day i in period j. The index counts the largest number of consecutive days where:

$$RR_{ij} < 1\text{mm}$$

2.0.6. CWD — Consecutive wet days

Maximum number of consecutive days with $RR \geq 1$ mm. Let RR_{ij} be the daily precipitation amount on day i in period j. The index is then defined as the largest number of consecutive days where:

$$RR_{ij} \geq 1mm$$

Table 3
Summary of the indices used in the analysis divided in three categories: indices related to the mean amount of precipitation, indices related to the intensity of precipitation and indices related with the frequency of precipitation.

Amount of precipitation	Intensity of precipitation	Frequency of rainfall
Annual total precipitation	Rx1day	CWDs
Seasonal mean precipitation	Rx2day	CDDs
Monthly mean precipitation	Rx5day	Wet days
Light rain	SDII	
Medium rain	R95pTOT	
Heavy rain		
Very heavy rain		

2.0.7. R95pTOT

Annual total precipitation when RR > 95^{th} percentile. Let RR_{wj} be the daily precipitation amount on a wet day in period i and let $RR_{wn}95$ be the 95^{th} percentile of precipitation on wet days w in the record. If W represents the number of wet days in the period, then:

$$R95_{pj} = \sum_{w=1}^{W} RR_{wj} \quad where \quad RR_{wj} > RR_{wn}95 \tag{4}$$

We also investigate trends in the annual number of days with rainfall in each of five categories:

2.0.8. Wet days

Annual count of days when daily precipitation is ≥ 1 mm. Let RR_{ij} be the daily precipitation amount on day i in period j. The number of wet days is then counted as the number of days when:

$$RR_{ij} \geq 1\text{mm} \tag{5}$$

2.0.9. Light rain

Annual count of days when daily precipitation is in the range ≥ 1 mm to 10 mm. Let RR_{ij} be the daily precipitation amount on day i in period j. The number of light rain days is then counted as the number of days where:

$$1\text{mm} \leq RR_{ij} \leq 10\text{mm} \tag{6}$$

2.0.10. Medium rain

Annual count of days when daily precipitation is in the range > 10 mm to 20 mm. Let RR_{ij} be the daily precipitation amount on day i in period j. The number of medium rain days is then counted as the number of days where:

$$10.1\text{mm} \leq RR_{ij} \leq 20\text{mm} \tag{7}$$

2.0.11. Heavy rain

Annual count of days when daily precipitation is in the range > 20 mm to 50 mm. Let RR_{ij} be the daily precipitation amount on day i in period j. The number of heavy rain days is then counted as the number of days where:

$$20.1\text{mm} \leq RR_{ij} \leq 50\text{mm} \tag{8}$$

2.0.12. Very heavy rain

Annual count of days when daily precipitation is greater than 50.1 mm. Let RR_{ij} be the daily precipitation amount on day i in period j. The number of very heavy rain days is then counted as the number of days where:

$$RR_{ij} > 50.1\text{mm} \tag{9}$$

Here we divide the indices into three categories (Table 3): indices related to the mean amount of precipitation, those related to precipitation intensity, and those related to rainfall frequency.

We employ the Mann–Kendall trend test, widely used in climatological analysis to detect trends (Wilks, 2019). The magnitude of each time series trend was determined using Sen's slope test (Atta-Ur and Muhammad, 2017). R-package "Trend" version 1.1.4 (Pohlert, 2020) was used to perform Mann–Kendall and Sen's slope tests. The version of the Mann–Kendall test implemented in this package works only on complete time series (i.e., without missing data), which was ensured by the removal of the incomplete years as described above.

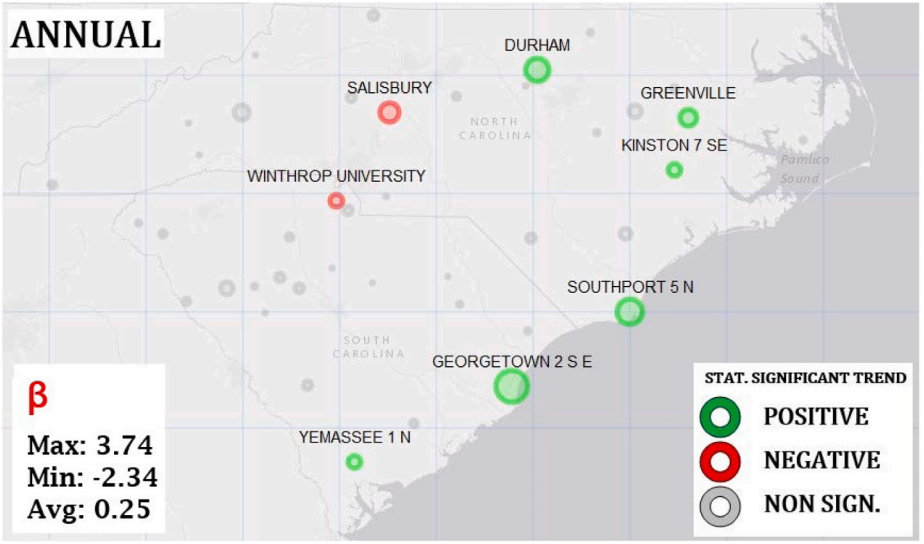

Fig. 2. Annual mean precipitation trends for every station with 95% of confidence level. Radius scale is proportional to Sen's slope estimator β (mm/year); stations with green markers present positive significant trend, stations with red markers present negative significant trend, while gray markers show stations with no significant trend. The legend in the bottom left corner shows the maximum, minimum, and average value of β. (For interpretation of the references to color in this figure legend, the reader is referred to the web version of this article.)

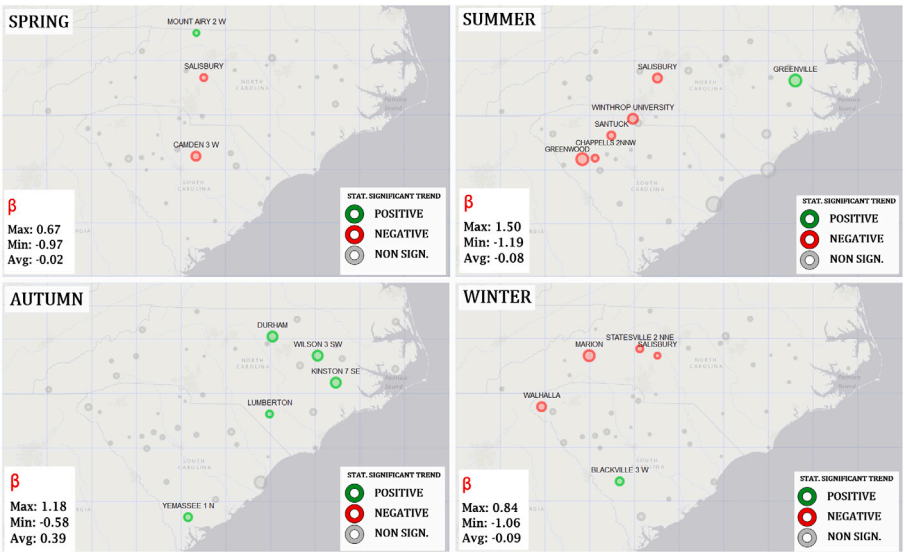

Fig. 3. Seasonal mean precipitation trends for every station during every season with 95% of confidence level. Radius scale is proportional to Sen's slope estimator β (mm/day); stations with green markers present positive significant trend, stations with red markers present negative significant trend, while grey markers show stations with no significant trend. The legend in the bottom left corner shows the maximum, minimum, and average value of β. (For interpretation of the references to color in this figure legend, the reader is referred to the web version of this article.)

3. Results and discussion

Eight of forty-four stations show a significant trend in total annual precipitation. Six of these show an increasing trend and are mostly located in the coastal region; two with decreasing trends are found in the central region (Fig. 2). Likewise, most stations show no trend in seasonal precipitation totals and, in general, there is no overlap between the detection of seasonal and annual trends (Fig. 3). Only three stations showed a trend in spring — two decreasing, one increasing. Five significant decreasing trends in summer were detected in the central region, four significant decreasing trends were found in the upstate area during winter. Only five stations showed a significant increasing trend in autumn, contrary to the autumn precipitation increases found by others investigating larger portions of the southeastern United States that excluded the Carolinas (Bishop et al., 2019).

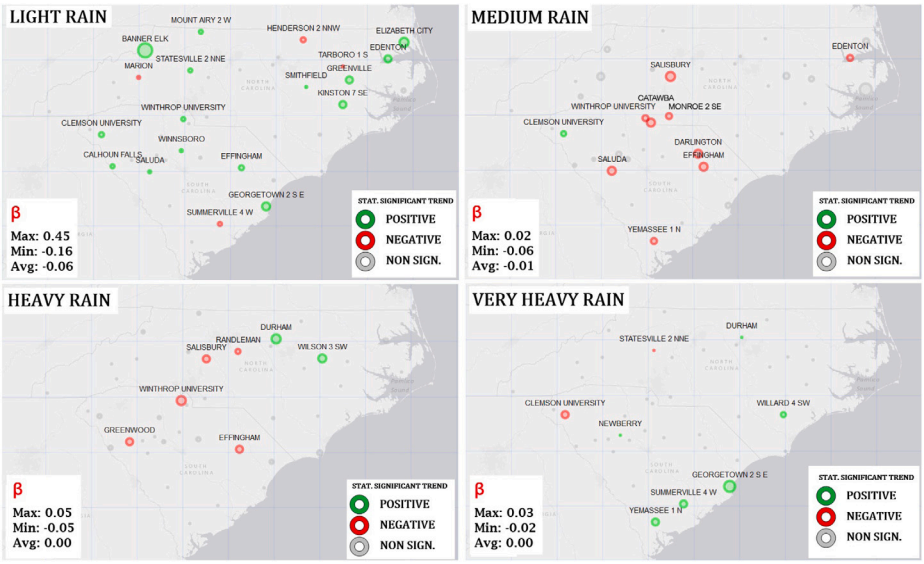

Fig. 4. Four categories of rain trends for every station with 95% of confidence level. Radius scale is proportional to Sen's slope estimator β (days/year); stations with green markers present significant positive trend, stations with red markers present significant negative trend, while grey markers show stations with no significant trend. The legend in the bottom left corner shows the maximum, minimum, and average value of β. (For interpretation of the references to color in this figure legend, the reader is referred to the web version of this article.)

Fifteen stations (34%) show a significant increasing trend in the number of "light" rain (1–10 mm) days; they are scattered across the entire study area (Fig. 4). Four stations, also widely scattered, show a significant decreasing trend in light rain days. The stations showing a significant trend in light rain nearly match the stations that show a significant trend in the number of wet days (Fig. 5). These results echo those showing large spatial variability in observed precipitation intensity [e.g., Qian et al., 2010] and suggesting compensation across the precipitation distribution at the global scale [e.g., Thackeray et al., 2018]. Nine stations have a significant decrease in "medium" rain (10–20 mm) events; only Clemson, SC, shows a significant increasing trend. "Heavy" rain events (20–50 mm) significantly decreased at five stations in the coastal plain or piedmont; two had an increasing trend. Days with rainfall amounts exceeding 50 mm ("very heavy" rain) increased significantly at four coastal and two central sites and decreased at two upstate sites. This last result does not appear related to the frequency of tropical systems in the last two decades, but is in agreement with Brown et al. (2020) who found similar patterns analyzing a broader region in the SEUS and suggested their potential relation with changes in the frequency of faster-moving frontal events or to droughts impacting the area. We conducted preliminary analysis for all stations from their initial year through 2000, and again using only 1950–2019 data to test sensitivity to time period. Both tests revealed only minor differences from the trends for the entire period of record. All things being equal, the lack of trends in seasonal or annual precipitation, combined with a shift in "light rain" events would decrease flooding risks.

Mean values of the simple precipitation intensity index (SDII), the ratio of daily precipitation amount on wet days to the number of wet days, are typically highest in coastal regions during summer and fall, and in the upstate during fall and winter (Supplementary materials, Fig. 2S). We found SDII trends in 23 to 39% of all stations examined, depending on season (Fig. 6). These trends are mixed in spring and fall, but during summer and particularly winter there is a clear trend of decreasing precipitation intensity as measured by SDII. As evidenced by the black circles enclosing the common clusters between the two different indices, there is a strong correlation between those stations experiencing this decreased intensity and those that show an increasing trend in the number of light rain days, a pattern most clearly seen in winter (Fig. 7). In fall and winter, we find a related correlation between increasing trends in wet days and increasing light rain days (Fig. 8).

Only 11% to 23% of stations exhibited a significant trend in consecutive wet days (CWD); these trends were dependent on season and typically not of the same sign (Fig. 9). In spring and winter, we found a nearly equal number of stations with increasing or decreasing trends. While only a fraction of all stations had a significant trend, the pattern was more consistent in summer, when the number of CWD significantly decreased at ten stations, and in fall, when it significantly increased at eight stations. Mean consecutive dry days (CDD) are greatest in autumn. It is also the season with the highest number of stations (41%) experiencing decreasing trends (Fig. 10). A clear pattern of decreasing trends, albeit at fewer stations, also occurs in spring (18% of all stations) and winter (20% of all stations). By contrast, CDD has changed less in summer — four stations had increasing trends, one had a decreasing trend. While the summer decrease in CWD at ten stations conforms to some empirical and modeling results suggesting decreasing duration of rain events (Powell and Keim, 2015; Giorgi et al., 2011), our results in other seasons do not provide such evidence, and, in fact, they are generally opposite to those suggesting longer stretches of dry days (Giorgi et al., 2011; Trenberth, 2011). Our results also differ from those of (Powell and Keim, 2015), who found an increase in dry spells in the Carolinas. Our results for individual seasons show decreasing CDD trends in winter, spring, and fall, with only a few stations showing an increase in summer.

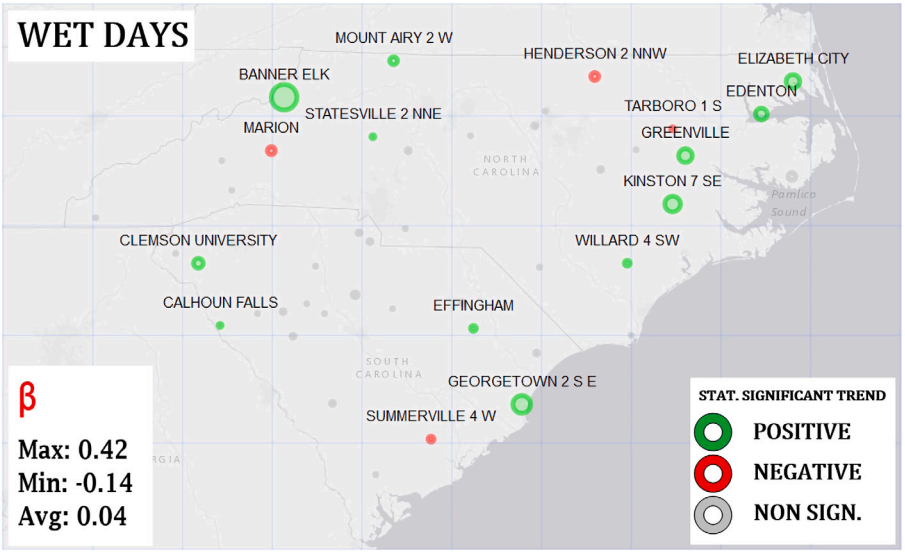

Fig. 5. Wet Days trends for every station with 95% of confidence level. Radius scale is proportional to Sen's slope estimator β (days/year); stations with green markers present positive significant trend, stations with red markers present negative significant trend while, grey markers show stations with no significant trend. The legend in the bottom left corner shows the maximum, minimum, and average value of β. (For interpretation of the references to color in this figure legend, the reader is referred to the web version of this article.)

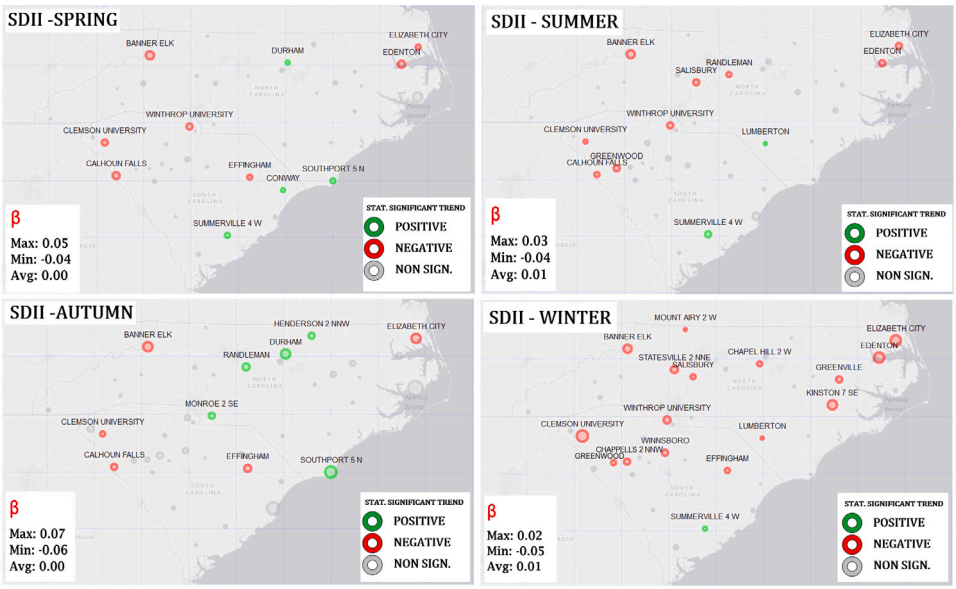

Fig. 6. SDII (Simple precipitation intensity index) trends for every station with 95% of confidence level in every season. Radius scale is proportional to Sen's slope estimator β (mm/day); stations with green markers present positive significant trend, stations with red markers present negative significant trend, while grey markers show stations with no significant trend. The legend in the bottom left corner shows the maximum, minimum, and average value of β. (For interpretation of the references to color in this figure legend, the reader is referred to the web version of this article.)

We measured seasonal maximum 1-, 2-, and 5-day precipitation values in order to account for time of observation differences and storms of different duration. Seasonal maxima for these intervals was greatest across the Carolinas in summer and fall. For 1-day maxima, high values span across the entire area in fall, and are more concentrated near the coast in summer. At 2-days, the highest values are typically near the coast during summer and fall. At 5-days, the highest values are spread uniformly across the region in summer and fall, and more concentrated at higher elevation sites in winter and spring (Supplementary materials, Fig. 3S, 4S, 5S). Few stations had a significant trend in 1-, 2-, and 5-day seasonal maxima. Typically, only 10% of stations had a significant increasing trend. About 20% of the stations had a significant increasing trend in 5-day maxima during fall, the most of any season and of the three aggregation periods (Fig. 11). Such trends have potential impacts on flood risk and for water supply management,

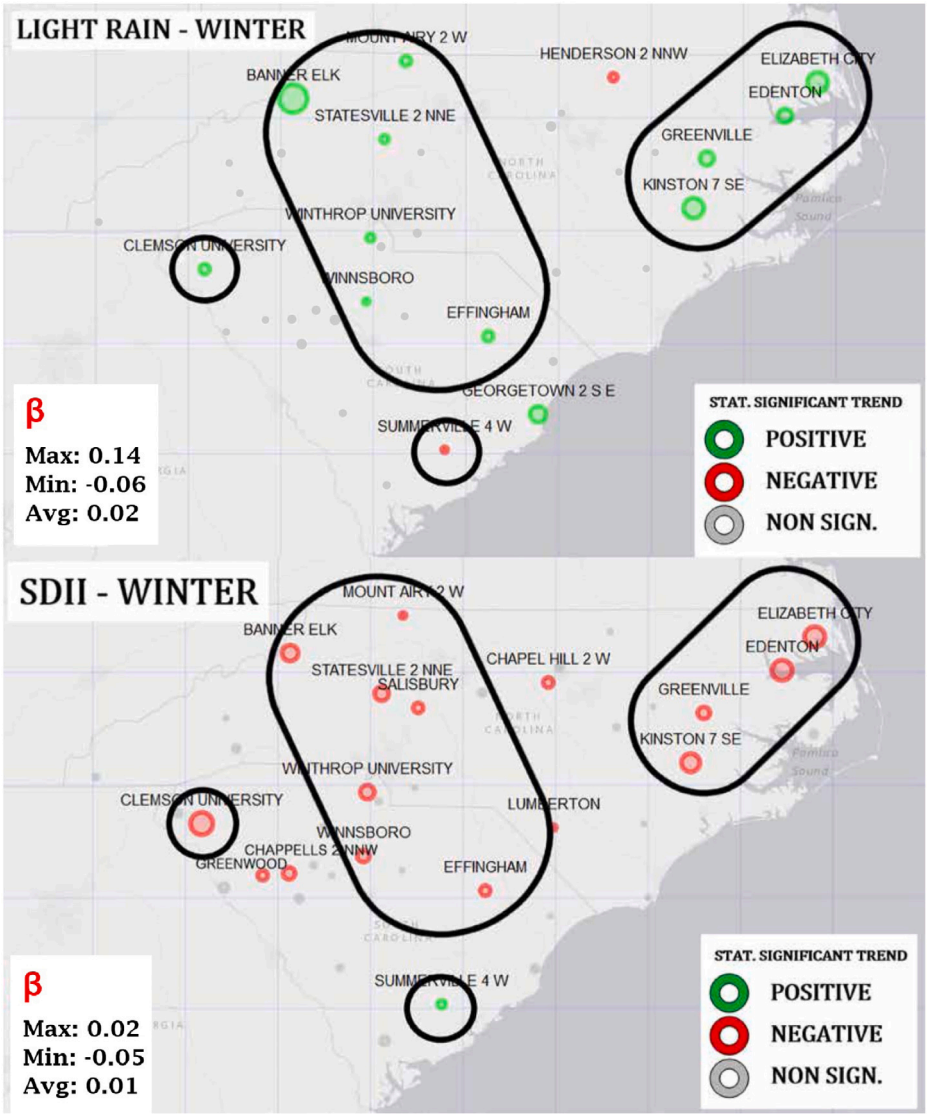

Fig. 7. Light rain and SDII trends for every station with 95% of confidence level during winter. Radius scale is proportional to Sen's slope estimator β (days/year) for light rain and (mm/day) for SDII; stations with green markers present positive significant trend, stations with red markers present significant negative trend, while grey markers show stations with no significant trend. The legend in the bottom left corner shows the maximum, minimum, and average value of β. Black circles in the figures enclose the common clusters between the two different indices. (For interpretation of the references to color in this figure legend, the reader is referred to the web version of this article.)

particularly for river basins where the practice of drawing down some reservoirs in fall could add additional flooding in the coastal plain. A handful of stations exhibited decreasing trends, mostly in summer or winter.

There also were very few stations that had significant trends in the 95th-percentile of 1-day rainfall accumulation on wet days. Four stations had increasing trends in spring, one in summer, two in fall; none of these trends was repeated for the same station across different seasons. In winter, five stations had significant decreasing trends; none had a significant increasing trend.

4. Summary

Our analysis of century-long precipitation records from forty-four USHCN stations in the Carolinas reveals relatively few consistent and statistically significant trends across the suite of ETCCDI measures of precipitation amount, frequency, and intensity. For individual stations, significant trends in a particular variable were not consistent across seasons, and a significant trend found in one variable was often absent in another similar variable (e.g., 95th-percentile events, vs. annual 1-day maxima). In addition, most trends had little in common spatially. One exception includes an increase in light precipitation in fall and winter which was positively

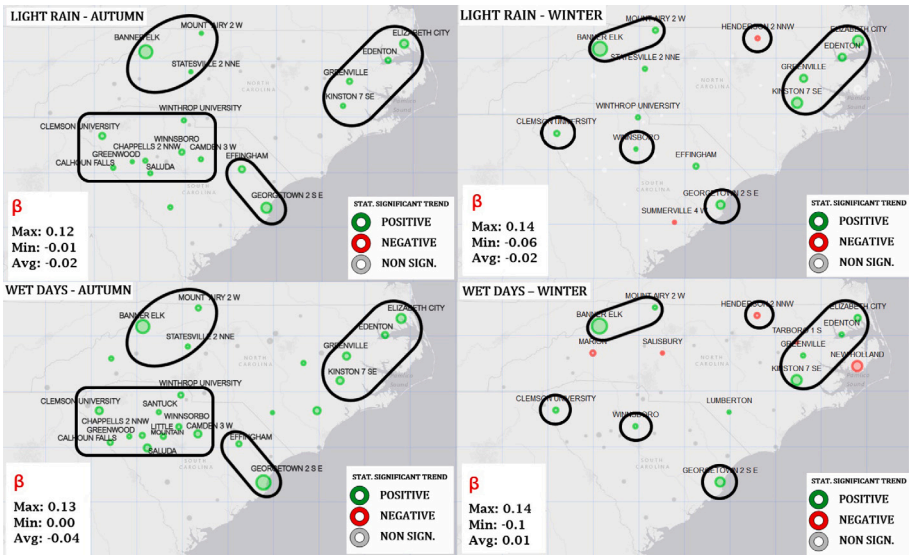

Fig. 8. "Light rain" and "Wet days" trends for every station with 95% of confidence level during autumn and winter. Radius scale is proportional to Sen's slope estimator β (days/year); stations with green markers present positive significant trend, stations with red markers present negative significant trend, while grey markers show stations with no significant trend. The legend in the bottom left corner shows the maximum, minimum, and average value of β. Black circles in the figures enclose the common clusters between the two different indices. (For interpretation of the references to color in this figure legend, the reader is referred to the web version of this article.)

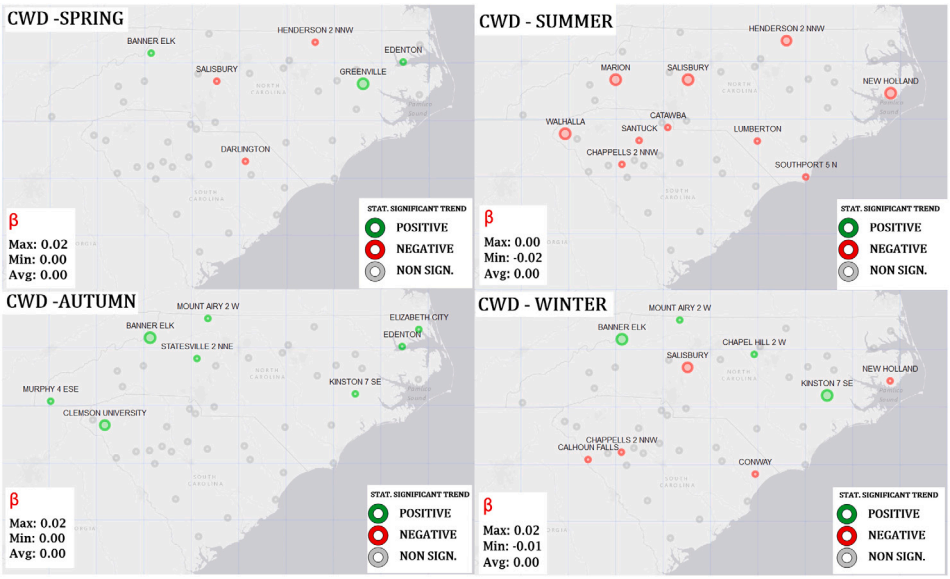

Fig. 9. Consecutive wet day trends for every station with 95% of confidence level in every season. Radius scale is proportional to Sen's slope estimator β (days/year); stations with green markers present positive significant trend, stations with red markers present negative significant trend while grey markers show stations with no significant trend. The legend in the bottom left corner shows the maximum, minimum, and average value of β. (For interpretation of the references to color in this figure legend, the reader is referred to the web version of this article.)

correlated with number of wet days and negatively correlated with SDII. This correlation, presented in Fig. 8, was investigated using a Pearson test with a 95% confidence level. This analysis resulted in a statistically significant relationship across all stations with a test statistic of 56.0% (confidence intervals = 54.0% to 58.1%). The same test confirmed statistically significant correlation between light rain and SDII (Fig. 7). Respectively, we estimated a significant correlation of 83% (confidence interval with $\alpha = 0.05$ from 81.4% to 83.3%) during autumn between light rain and wet days and a correlation of 78.7% (confidence interval from 77.5% to 79.8%) between the same indices during winter. The lack of trends in precipitation amount or intensity contrasts with previous work examining a broader swath of the southeastern United States that documents regional increases in precipitation intensity (Karl

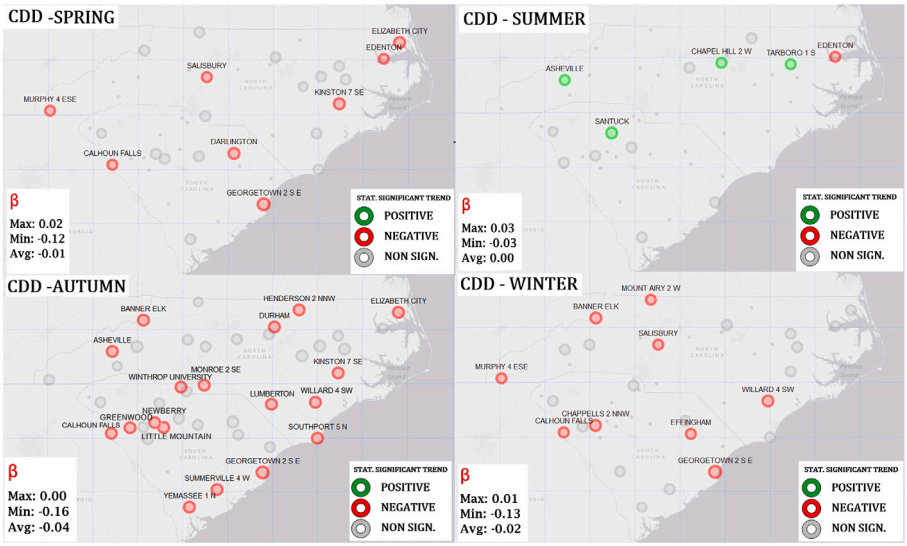

Fig. 10. Consecutive dry day trends for every station with 95% of confidence level in every season. Radius scale is proportional to Sen's slope estimator β (days/year); stations with green markers present positive significant trend, stations with red markers present negative significant trend while grey markers show stations with no significant trend. The legend in the bottom left corner shows the maximum, minimum, and average value of β. (For interpretation of the references to color in this figure legend, the reader is referred to the web version of this article.)

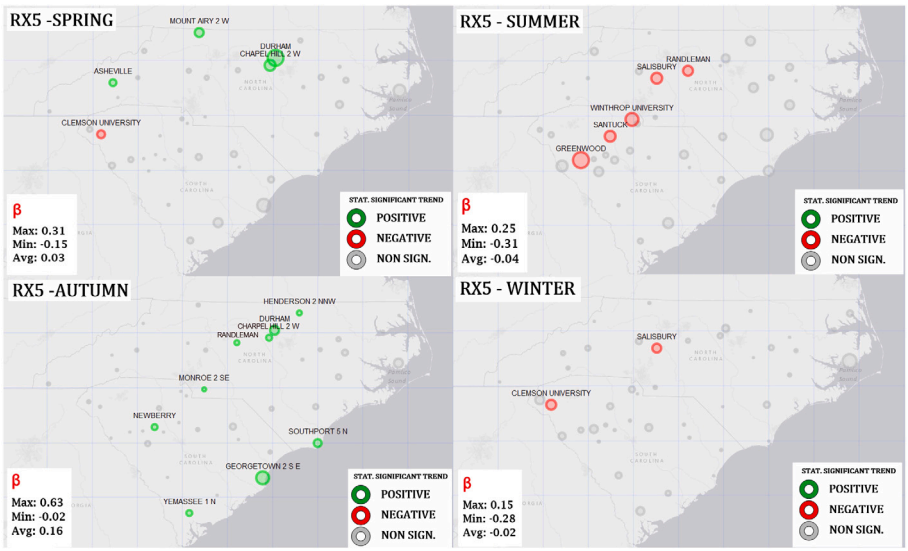

Fig. 11. Rx5 (Seasonal maximum 5-day precipitation) trends for every station with 95% of confidence level in every season. Radius scale is proportional to Sen's slope estimator beta; stations with green markers present positive significant trend, stations with red markers present negative significant trend, while grey markers show stations with no significant trend. The legend in the bottom left corner shows the maximum, minimum, and average value of β. (For interpretation of the references to color in this figure legend, the reader is referred to the web version of this article.)

and Knight, 1998; Easterling et al., 2017; Kunkel et al., 2020b). Our findings do conform, however, to those studies that distinguish trends within the region and, in particular, suggest a more complicated and/or less robust signal in the Carolinas (Powell and Keim, 2015; Brown et al., 2019; Skeeter et al., 2018; Brown et al., 2020; Kunkel et al., 2020a). Amidst the subtle and mixed signals of precipitation trends in the Carolinas, a few conclusions emerge from our analysis. First, about one third of the stations examined show an increase in light rain. This is correlated with an increasing number of wet days and decreasing precipitation intensity as measured by SDII, an index that explicitly includes the number of wet days in its ratio. While beyond the scope of this paper, these findings may be related to changes in atmospheric circulation or aerosol concentration and composition affecting regional cloud processes and rain rates (Qian et al., 2010). Second, all other measures of precipitation intensity suggest that only a small portion of stations in the Carolinas (typically 10% or fewer) show any significant trend, and a few of these are decreasing. The most notable

exception is an increasing trend in the 2-day (14% of all stations) and 5-day (20% of all stations) fall maxima precipitation; this is also found in at least one other study (Janssen et al., 2016).

Our detailed look at a relatively small portion of the SEUS allowed us to investigate a longer time frame, more stations, and a wider range of precipitation measures than many other studies of the region. The long period of record includes a range of interannual and interdecadal variability. This was evident in many of the ETCCDI measures investigated and made trend detection more difficult. Others have noted the complexity of the SEUS precipitation record, guided by tropical ocean variability linked to the El Niño/Southern Oscillation (Ropelewski and Halpert, 1986; Kiladis and Diaz, 1989; Ropelewski and Halpert, 1989), internal variability associated with the North Atlantic subtropical high, sea-surface temperatures, and other drivers (Seager et al., 2009; Hoerling et al., 2010; Li et al., 2012; Diem, 2013; Kam et al., 2014; Park Williams et al., 2017; Ferreira and Rickenbach, 2021; Nieto Ferreira and Rickenbach, 2020), as well as interdecadal modulations like the Atlantic Multidecadal Oscillation (Enfield et al., 2001; Gregersen et al., 2014; Hodgkins et al., 2017). Given that some studies have shown trends in the region for shorter periods, our results suggest that such trends could depend on record length. Future work could address this issue directly. One limitation of the long time series is that data sparsity restricts thorough investigation into thermodynamic or dynamic drivers that might influence trends. Future analysis could investigate statistical relationships between precipitation variability and longer-term indices of ENSO and the AMO.

Our analysis considering a longer time frame, more stations, and a wider range of measures contributes to a broader understanding of precipitation changes in the Carolinas. These findings provide a baseline for future climatological investigation, but also have relevance for adaptation planning. Many communities in the Carolinas have experienced increased flooding in recent years despite the fact that precipitation trends have been subtle. Since increased flooding could result from multiple factors (e.g., precipitation amount and intensity, land-use change in a rapidly growing part of the country, sea-level rise in coastal environments), adaptation effectiveness demands an understanding of the relative importance of underlying processes. While our analysis shows limited trends in precipitation measures, concerns and preparation for future changes are prudent. The region likely will experience higher air temperatures which will increase moisture availability (Kunkel et al., 2020a). Moreover, increasing Atlantic and Gulf of Mexico sea-surface temperatures will likely fuel evaporation rates for extratropical, convective, and tropical systems that produce heavy precipitation events. In addition to these thermodynamic drivers, precipitation changes could be driven by dynamic forces, particularly due to an enhanced North Atlantic subtropical high (Lopez-Cantu and Samaras, 2018; Bishop et al., 2019). In a region that regularly experiences profound impacts of interannual precipitation variability on human and physical systems, potential changes in the drivers of hydroclimate extremes warrants attention in the next decades.

Acknowledgments

The authors would like to thank: the National Centers for Environmental Information (NOAA) for their work to create, improve, and maintain the USHCN network, the dataset on which this work is based; Prof. Federico Porcù from the Department of Physics and Astronomy ‘‘Augusto Righi’’ of the University of Bologna for his thorough review of the work in its initial stages; the R community and all contributors to the R packages used here, and to OpenStreet Map. This research was supported by supported by the National Oceanic and Atmospheric Administration (NOAA) Climate Program Office (grant no. NA16OAR4310163).

Appendix A. Supplementary data

Supplementary material related to this article can be found online at https://doi.org/10.1016/j.ejrh.2022.101201.

References

Alexander, L., Fowler, H., Bador, M., Behrangi, A., Donat, M., Dunn, R., Funk, C., Goldie, J., Lewis, E., Rogé, M., Seneviratne, S., Venugopal, V., 2019. On the use of indices to study extreme precipitation on sub-daily and daily timescales. Environ. Res. Lett. 14 (12), 125008. http://dx.doi.org/10.1088/1748-9326/ab51b6.

Alexander, L., Hope, P., Collins, D., Trewin, B., Lynch, A., Nicholls, N., 2007. Trends in Australia’s climate means and extremes: A global context. Aust. Meteorol. Mag. 56 (1), 1–18, https://citeseerx.ist.psu.edu/viewdoc/download?doi=10.1.1.222.5972&rep=rep1&type=pdf.

Alexander, L., Zhang, X., Peterson, T., Caesar, J., BA, G., Tank, A., Haylock, M., Collins, D., Trewin, B., Rahimzadeh, F., Tagipour, A., Kumar, K., Revadekar, J., Griffiths, G., Vincent, L., Stephenson, D., Burn, J., Aguilar, E., Brunet, M., Vazquez-Aguirre, J., 2006. Global observed changes in daily climate extremes of temperature and precipitation. J. Geophys. Res. 111 (D5), http://dx.doi.org/10.1029/2005JD006290.

Atta-Ur, R., Muhammad, D., 2017. Spatio-statistical analysis of temperature fluctuation using Mann-Kendall and Sen’s slope approach. Clim. Dynam. 48, 783–797. http://dx.doi.org/10.1007/s00382-016-3110-y.

Bishop, D.A., Williams, A.P., Seager, R., Fiore, A.M., Cook, B.I., Mankin, J.S., Singh, D., Smerdon, J.E., Rao, M.P., 2019. Investigating the causes of increased twentieth-century fall precipitation over the southeastern United States. J. Clim. 32 (2), 575–590. http://dx.doi.org/10.1175/JCLI-D-18-0244.1.

Bonnin, G., Maitaria, K., Yekta, M., 2011. Trends in rainfall exceedances in the observed record in selected areas of the United States. J. Am. Water Resour. Assoc. 47, 1173–1182. http://dx.doi.org/10.1111/j.1752-1688.2011.00603.x.

Brown, V.M., Keim, B.D., Black, A.W., 2019. Climatology and trends in hourly precipitation for the southeast United States. J. Hydrometeorol. 20 (8), 1737–1755. http://dx.doi.org/10.1175/JHM-D-19-0004.1.

Brown, V.M., Keim, B.D., Black, A.W., 2020. Trend analysis of multiple extreme hourly precipitation time series in the southeastern United States. J. Appl. Meteorol. Climatol. 59 (3), 427–442. http://dx.doi.org/10.1175/JAMC-D-19-0119.1.

Diem, J., 2013. Influences of the bermuda high and atmospheric moistening on changes in summer rainfall in the Atlanta, Georgia region, USA. Int. J. Climatol. 33 (1), 160–172. http://dx.doi.org/10.1002/joc.3421.

Easterling, D.R., Kunkel, K.E., Arnold, J.R., Knutson, T., LeGrande, A.N., Leung, L.R., Vose, R.S., Waliser, D.E., Wehner, M.F., 2017. Precipitation change in the United States. In: Wuebbles, D.J., Fahey, D.W., Hibbard, K.A., Dokken, D.J., Stewart, B.C., Maycock, T.K. (Eds.), Climate Science Special Report: Fourth National Climate Assessment, Vol. I. U.S. Global Change Research Program, Washington, D.C., pp. 207–230. http://dx.doi.org/10.7930/J0H993CC.

Easterling, K.K., Young, R., Hennon, Y., 2013. Probable maximum precipitation and climate change. Geophys. Res. Lett. 40 (7), 1402–1408. http://dx.doi.org/10.1002/grl.50334.

Enfield, D.B., Mestas-Nuñez, A.M., Trimble, P.J., 2001. The atlantic multidecadal oscillation and its relation to rainfall and river flows in the continental U.S.. Geophys. Res. Lett. 28 (10), 2077–2080. http://dx.doi.org/10.1029/2000GL012745.

Ferreira, R.N., Rickenbach, T.M., 2021. Mechanisms for springtime onset of isolated precipitation across the southeastern United States. Atmosphere 12 (2), http://dx.doi.org/10.3390/atmos12020213.

Fischer, E., Knutti, R., 2015. Anthropogenic contribution to global occurrence of heavy-precipitation and high-temperature extremes. Nature Clim. Change 5, http://dx.doi.org/10.1038/NCLIMATE2617.

Forestieri, A., Lo Conti, F., Blenkinsop, S., Cannarozzo, M., Fowler, H.J., Noto, L.V., 2018. Regional frequency analysis of extreme rainfall in Sicily (Italy). Int. J. Climatol. 38 (S1), e698–e716. http://dx.doi.org/10.1002/joc.5400.

Gershunov, A., Barnett, T.P., 1998. Interdecadal modulation of ENSO teleconnections. Bull. Am. Meteorol. Soc. 79 (12), 2715–2726. http://dx.doi.org/10.1175/1520-0477(1998)079<2715:IMOET>2.0.CO;2.

Giorgi, F., Im, E.-S., Coppola, E., Diffenbaugh, N.S., Gao, X.J., Mariotti, L., Shi, Y., 2011. Higher hydroclimatic intensity with global warming. J. Clim. 24 (20), 5309–5324. http://dx.doi.org/10.1175/2011JCLI3979.1.

Grabowski, W.W., 2019. Separating physical impacts from natural variability using piggybacking (master-slave) technique. Adv. Geosci. 49, 105–111. http://dx.doi.org/10.5194/adgeo-49-105-2019.

Gregersen, I., Madsen, H., Rosbjerg, D., Arnbjerg-Nielsen, K., 2014. Long term variations of extreme rainfall in Denmark and southern Sweden. Clim. Dynam. 44 (44), 3155–3169. http://dx.doi.org/10.1007/s00382-014-2276-4.

Hodgkins, G., Whitfield, P., Burn, D., Hannaford, J., Renard, B., Stahl, K., Fleig, A., Madsen, H., Mediero, L., Korhonen, J., Murphy, C., Wilson, D., 2017. Climate-driven variability in the occurrence of major floods across North America and Europe. J. Hydrol. 552, 704–717. http://dx.doi.org/10.1016/j.jhydrol.2017.07.027.

Hoerling, M., Eischeid, J., Perlwitz, J., 2010. Regional precipitation trends: Distinguishing natural variability from anthropogenic forcing. J. Clim. 23 (8), 2131–2145. http://dx.doi.org/10.1175/2009JCLI3420.1.

Huang, H., Winter, J.M., Osterberg, E.C., Horton, R.M., Beckage, B., 2017. Total and extreme precipitation changes over the Northeastern United States. J. Hydrometeorol. 18 (6), 1783–1798. http://dx.doi.org/10.1175/JHM-D-16-0195.1.

IPCC, 2012. Managing the Risks of Extreme Events and Disasters to Advance Climate Change Adaptation. Cambridge University Press, Cambridge, UK, and New York, NY, USA, p. 582, URL: https://www.ipcc.ch/report/managing-the-risks-of-extreme-events-and-disasters-to-advance-climate-change-adaptation/. (Last accessed 04 January 2021),

Ivancic, T., Shaw, S., 2016. A U.S.-based analysis of the ability of the Clausius-Clapeyron relationship to explain changes in extreme rainfall with changing temperature. J. Geophys. Res.: Atmos. 121 (7), 3066–3078. http://dx.doi.org/10.1002/2015JD024288.

Janssen, E., Sriver, R., Wuebbles, D., Kunkel, K., 2016. Seasonal and regional variations in extreme precipitation event frequency using CMIP5. Geophys. Res. Lett. 43 (10), 5385–5393. http://dx.doi.org/10.1002/2016GL069151.

Kam, J., Sheffield, J., Wood, E.F., 2014. A multiscale analysis of drought and pluvial mechanisms for the southeastern United States. J. Geophys. Res.: Atmos. 119 (12), 7348–7367. http://dx.doi.org/10.1002/2014JD021453.

Karl, T., Knight, R., 1998. Secular trends of precipitation amount, frequency, and intensity in the United States. Bull. Am. Meteorol. Soc. 79 (2), 231–242. http://dx.doi.org/10.1175/1520-0477(1998)079<0231:STOPAF>2.0.CO;2.

Kiladis, G.N., Diaz, H.F., 1989. Global climatic anomalies associated with extremes in the southern oscillation. J. Clim. 2 (9), 1069–1090. http://dx.doi.org/10.1175/1520-0442(1989)002<1069:GCAAWE>2.0.CO;2.

Knight, D.B., Davis, R.E., 2009. Contribution of tropical cyclones to extreme rainfall events in the southeastern United States. J. Geophys. Res.: Atmos. 114 (D23), http://dx.doi.org/10.1029/2009JD012511.

Konrad, C.E., 2001. The most extreme precipitation events over the eastern United States from 1950 to 1996: Considerations of scale. J. Hydrometeorol. 2 (3), 309–325. http://dx.doi.org/10.1175/1525-7541(2001)002<0309:TMEPEO>2.0.CO;2.

Konrad, C., Perry, B., 2009. Relationships between tropical cyclones and heavy rainfall in the Carolina region of the USA. Int. J. Climatol. 30, 522–534. http://dx.doi.org/10.1002/joc.1894.

Kunkel, K.E., Easterling, D.R., Kristovich, D.A.R., Gleason, B., Stoecker, L., Smith, R., 2012. Meteorological causes of the secular variations in observed extreme precipitation events for the conterminous United States. J. Hydrometeorol. 13 (3), 1131–1141. http://dx.doi.org/10.1175/JHM-D-11-0108.1.

Kunkel, K.E., Karl, T.R., Squires, M.F., Yin, X., Stegall, S.T., Easterling, D.R., 2020a. Precipitation extremes: Trends and relationships with average precipitation and precipitable water in the contiguous United States. J. Appl. Meteorol. Climatol. 59 (1), 125–142. http://dx.doi.org/10.1175/JAMC-D-19-0185.1.

Kunkel, K., Stevens, S., Stevens, L., Karl, T., 2020b. Observed climatological relationships of extreme daily precipitation events with precipitable water and vertical velocity in the contiguous United States. Geophys. Res. Lett. 47 (12), http://dx.doi.org/10.1029/2019GL086721, e2019GL086721.

Li, L., Li, W., Kushnir, Y., 2012. Variation of North Atlantic subtropical high western ridge and its implication to the southeastern US summer precipitation. Clim. Dynam. 39, 1401–1412. http://dx.doi.org/10.1007/s00382-011-1214-y.

Lopez-Cantu, T., Samaras, C., 2018. Temporal and spatial evaluation of stormwater engineering standards reveals risks and priorities across the United States. Environ. Res. Lett. 13 (7), 074006. http://dx.doi.org/10.1088/1748-9326/aac696.

Menne, M., N., W.J.C., S., V.R., 2006. U.S. historical climatology Network (USHCN): Daily temperature precipitation and snow data. http://dx.doi.org/10.3334/CDIAC/CLI.NDP070.

Nieto Ferreira, R., Rickenbach, T.M., 2020. Effects of the north atlantic subtropical high on summertime precipitation organization in the southeast United States. Int. J. Climatol. 40 (14), 5987–6001. http://dx.doi.org/10.1002/joc.6561.

NOAA, 2021. US historical climatology network (USHCN). URL: https://www.ncdc.noaa.gov/data-access/land-based-station-data/land-based-datasets/us-historical-climatology-network-ushcn. (Last accessed 04 January 2021).

O'Gorman, P.A., Schneider, T., 2009. The physical basis for increases in precipitation extremes in simulations of 21st-century climate change. Proc. Natl. Acad. Sci. 106 (35), 14773–14777. http://dx.doi.org/10.1073/pnas.0907610106.

Park Williams, A., Cook, B.I., Smerdon, J.E., Bishop, D.A., Seager, R., Mankin, J.S., 2017. The 2016 southeastern US drought: An extreme departure from centennial wetting and cooling. J. Geophys. Res.: Atmos. 122 (20), 10,888–10,905. http://dx.doi.org/10.1002/2017JD027523.

Pendergrass, A., 2018. What precipitation is extreme? Science 360 (6393), 1072–1073. http://dx.doi.org/10.1126/science.aat1871.

Pohlert, T., 2020. Non-parametric trend tests and change-point detection. pp. 2–8, URL: https://CRAN.R-project.org/package=trend. (Last Accessed 04 January 2021), R package version 1.1.4.

Powell, E.J., Keim, B.D., 2015. Trends in daily temperature and precipitation extremes for the southeastern United States: 1948–2012. J. Clim. 28 (4), 1592–1612. http://dx.doi.org/10.1175/JCLI-D-14-00410.1.

Qian, Y., Gong, D., Leung, R., 2010. Light rain events change over North America, Europe, and Asia for 1973–2009. Atmos. Sci. Lett. 11 (4), 301–306. http://dx.doi.org/10.1002/asl.298.

Ropelewski, C.F., Halpert, M.S., 1986. North American precipitation and temperature patterns associated with the El Niño/Southern Oscillation (ENSO). Mon. Weather Rev. 114 (12), 2352–2362. http://dx.doi.org/10.1175/1520-0493(1986)114<2352:NAPATP>2.0.CO;2.

Ropelewski, C.F., Halpert, M.S., 1989. Precipitation patterns associated with the high index phase of the southern oscillation. J. Clim. 2 (3), 268–284. http://dx.doi.org/10.1175/1520-0442(1989)002<0268:PPAWTH>2.0.CO;2.

Seager, R., Tzanova, A., Nakamura, J., 2009. Drought in the southeastern United States: Causes, variability over the last millennium, and the potential for future hydroclimate change. J. Clim. 22 (19), http://dx.doi.org/10.1175/2009JCLI2683.1.

Shepherd, M., Grundstein, A., Mote, T., 2007. Quantifying the contribution of tropical cyclones to extreme rainfall along the coastal southeastern United States. Geophys. Res. Lett. 34 (23), L23810. http://dx.doi.org/10.1029/2007GL031694.

Skeeter, W., Senkbeil, J., Keellings, D., 2018. Spatial and temporal changes in the frequency and magnitude of intense precipitation events in the southeastern United States. Int. J. Climatol. 39, 768–782. http://dx.doi.org/10.1002/joc.5841.

Tabari, 2020. Climate change impact on flood and extreme precipitation increases with water availability. Sci. Rep. 10 (1), http://dx.doi.org/10.1038/s41598-020-70816-2.

Thackeray, C.W., DeAngelis, A.M., Hall, A., Swain, D.L., Qu, X., 2018. On the connection between global hydrologic sensitivity and regional wet extremes. Geophys. Res. Lett. 45 (20), 11,343–11,351. http://dx.doi.org/10.1029/2018GL079698.

Trenberth, K., 2011. Changes in precipitation with climate change. Clim. Res. 47, 123–138. http://dx.doi.org/10.3354/cr00953.

Trenberth, K.E., Dai, A., Rasmussen, R.M., Parsons, D.B., 2003. The changing character of precipitation. Bull. Am. Meteorol. Soc. 84 (9), 1205–1218. http://dx.doi.org/10.1175/BAMS-84-9-1205.

Wilks, D.S., 2019. Statistical Methods in the Atmospheric Sciences. Elsevier.

Zhang, X., Alexander, L., Hegerl, G.C., Jones, P., Tank, A.K., Peterson, T.C., Trewin, B., Zwiers, F.W., 2011a. Indices for monitoring changes in extremes based on daily temperature and precipitation data. WIREs Climate Change 2 (6), 851–870. http://dx.doi.org/10.1002/wcc.147.

Zhang, Y.X., Sun, S., Olsen, S.C., Dubey, M.K., He, J.H., 2011b. CCSM3 simulated regional effects of anthropogenic aerosols for two contrasting scenarios: Rising Asian emissions and global reduction of aerosols. Int. J. Climatol. 31 (1), 95–114. http://dx.doi.org/10.1002/joc.2060.

Zhang, X., Zwiers, F.W., Li, G., Wan, H., Cannon, A.J., 2017. Complexity in estimating past and future extreme short-duration rainfall. Nat. Geosci. 10 (4), 255–259. http://dx.doi.org/10.1038/ngeo2911.